Aluminophosphate Membranes

DOI: 10.1002/anie.201108042

Oriented CoSAPO-5 Membranes by Microwave-Enhanced Growth on TiO_2-Coated Porous Alumina**

*Jared A. Stoeger, Miguel Palomino, Kumar Varoon Agrawal, Xueyi Zhang, Georgios N. Karanikolos, Susana Valencia, Avelino Corma, and Michael Tsapatsis**

Supported polycrystalline films composed of microporous solid materials have been the subject of numerous reports over the last decade.[1–3] Specifically, methods have been developed for the design and processing of microporous zeolite membranes for high-resolution molecular selectivity.[4–6] Aluminophosphate-5 ($AlPO_4$-5, AFI zeolite structure type) is a class of microporous material comprising alternating AlO_4 and PO_4 tetrahedra forming a 12-membered ring framework with one-dimensional cylindrical pores aligned parallel to the crystallographic *c*-axis.[7] NMR evidence has suggested that one-dimensional channels impart significantly higher molecular mobility in $AlPO_4$-5 when compared to similarly sized zeolites with interconnected pore networks,[8] for example, a 1000-fold flux increase compared to the MFI zeolite type, though there have been limited reports using $AlPO_4$-5 as a molecular sieving membrane material. Those published have exemplified challenges in the development of supported AFI-type membranes: a multi-step process for the alignment of metal-embedded $AlPO_4$-5 crystals with a low ratio of crystal area to overall membrane area and hindering cost-effective scale-up,[9] crystalline misorientation limiting selective transport pathways,[10] and most recently, crystal densification and defect formation at temperatures necessary for membrane activation (removal of structure-directing agent molecules).[11] Although other methods have succeeded in the fabrication of preferentially oriented AFI-type films,[12–19] an examination of their quality through molecular separation performance has not yet been reported.

Following the initial discovery of $AlPO_4$-5, Lok et al. reported on the synthesis of silicoaluminophosphate-5 (SAPO-5), a structural analogue of $AlPO_4$-5 with a portion of the framework Al or P substituted by Si.[20] Subsequent studies have shown the effect of the growth method, reaction conditions, precursor contents, and metal substitution on the crystal morphology of AFI-type materials.[21–25] In particular, Jhung et al. investigated the microwave-assisted crystallization of plate-like SAPO-5 crystals through a manipulation of silica content in acidic or basic conditions.[26] Furthermore, Lai and co-workers assembled such crystals through manual assembly on a PVA-coated substrate, forming a uniform monolayer of plate-like SAPO-5 layers with a preferred *c*-orientation.[27]

The fabrication of a high-quality membrane relies on the control of essential film characteristics such as crystal orientation, intergrowth, and continuity as well as a contribution from the physical properties of the chosen support surface. Microwave-based hydrothermal reactions have been shown to rapidly fabricate metal–organic framework (MOF) thin films[28] and continuous *b*-oriented MFI films on stainless steel supports.[29] Hwang et al. revealed a method to pattern oriented silicalite-1 crystallites on the surface of metal oxide-coated substrates through microwave-enhanced growth.[30] It was postulated that surface hydroxy groups were selectively activated by microwave radiation, playing a significant role in the preferred orientation and degree of coverage of the silicalite-1 crystals.

Here, we report a facile method for the formation of preferentially *c*-out-of-plane-oriented cobalt-substituted SAPO-5 membranes (CoSAPO-5, AFI zeolite structure type) by selective microwave activation of a slip-coated TiO_2 layer on porous α-Al_2O_3 disc supports. In situ hydrothermal microwave growth resulted in an oriented plate-like crystal seed layer on the surface of the TiO_2 coating, which was followed by secondary hydrothermal microwave growth using a fresh precursor solution. Membrane fabrication and characterization details are given in the Supporting Information.

The microwave growth of aluminophosphate materials has been reported to reduce the hydrothermal crystallization time and improve crystal quality.[9,31] Furthermore, metal substitution was shown to reduce the aspect ratio through

[*] J. A. Stoeger,[+] K. V. Agrawal, X. Zhang, Prof. M. Tsapatsis
Department of Chemical Engineering and Materials Science
University of Minnesota, Minneapolis, MN 55455 (USA)
E-mail: tsapatsis@umn.edu
M. Palomino,[+] S. Valencia, Prof. A. Corma
Instituto de Tecnologia Quimica (CSIC-UPV)
Universidad Politecnica de Valencia
Avda de los Naranjos s/n 46022 Valencia (Spain)
G. N. Karanikolos
Institute of Physical Chemistry
Demokritos National Research Center, Athens 153 10 (Greece)
[+] These authors contributed equally to this work.

[**] We thank Dr. Christopher Lew for assistance with diffuse reflectance UV/Vis experiments. Support from the NSF (grant NSF-NIRT CMMI 0707610) and the Petroleum Institute of Abu Dhabi through the ADMIRE partnership (Abu Dhabi–Minnesota Institute for Research Excellence) is appreciated. M.P. acknowledges CSIC for a JAE doctoral fellowship, A.C. would like to thank CONSOLIDER Ingenio 2010-MULTICAT, and G.N.K. acknowledges a European Marie Curie International Reintegration Grant (FP7, grant agreement no. 210947). Portions of this work were carried out in the Nanofabrication Center, part of the National Nanotechnology Infrastructure Network (NNIN) which receives support from the NSF, and in the Characterization Facility on the campus of the University of Minnesota-Twin Cities which receives partial support from the NSF through the MRSEC program.

Supporting information for this article is available on the WWW under http://dx.doi.org/10.1002/anie.201108042.

inhibition of crystal growth along the elongated crystallographic *c*-axis.[23,26] Scanning electron microscopy (SEM, Figure 1a) and transmission electron microscopy (TEM, Figure 1b) images of as-synthesized CoSAPO-5 crystallites

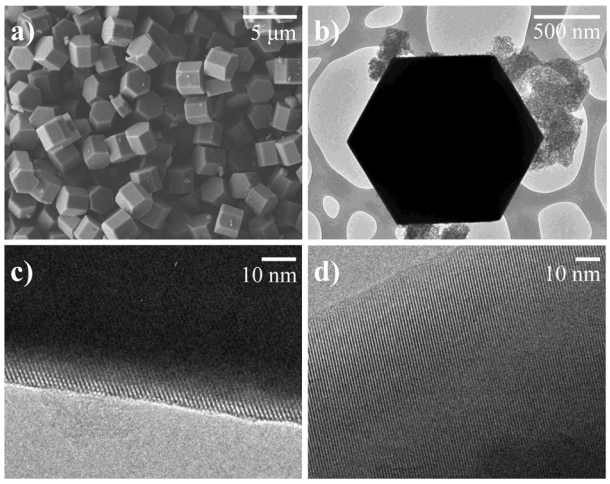

Figure 1. Images by a) SEM and b) low-magnification TEM highlight the crystalline CoSAPO-5 hexagonal prismatic morphology. High resolution TEM images of c) parallel and d) perpendicular alignment to the crystallographic *c*-axis reveal the one-dimensional pore structure.

show an evident hexagonal prismatic morphology. The one-dimensional pore structure of AFI-type materials is observed by high-resolution TEM imaging. In Figure 1c, the imaging direction is parallel to the crystallographic *c*-axis (i.e. the hexagonal face of the crystal), while the perpendicular imaging direction in Figure 1d highlights the non-interconnected straight channels. The elemental compositions of the unsupported CoSAPO-5 crystals before and after heat treatment are shown in the Supporting Information, Table S1.

As previously described for zeolite MFI films on dense supports,[30] selective microwave activation of a metal oxide surface may impart a preferential crystal orientation. The surface structure of a porous α-Al_2O_3 disc support used in the fabrication of CoSAPO-5 membranes is shown in Figure 2a. The preparation, slip-coating, and heat treatment of the TiO_2 layer in Figure 2b followed a report by Zaspalis et al.[32] and was furthermore used for the supported growth of CoSAPO-5. The in situ hydrothermal microwave growth of CoSAPO-5 resulted in the oriented crystalline seed layer in Figure 2c. A secondary hydrothermal microwave growth step (Figure 2d) was used to improve crystal intergrowth while retaining the original crystallographic orientation and thickness. Diffuse reflectance UV/Vis spectroscopy of a CoSAPO-5 membrane confirmed the incorporation of Co into the framework (Figure S1).

It is important to note that under identical growth conditions using only the bare α-Al_2O_3 support, the resulting seed layer is sparse and misoriented (Figure S2). Furthermore, an investigation into the TiO_2 coating process revealed that the propagation of defects and/or cracks in the TiO_2 layer reduces the CoSAPO-5 crystal surface coverage and increases misorientation following microwave growth. Therefore,

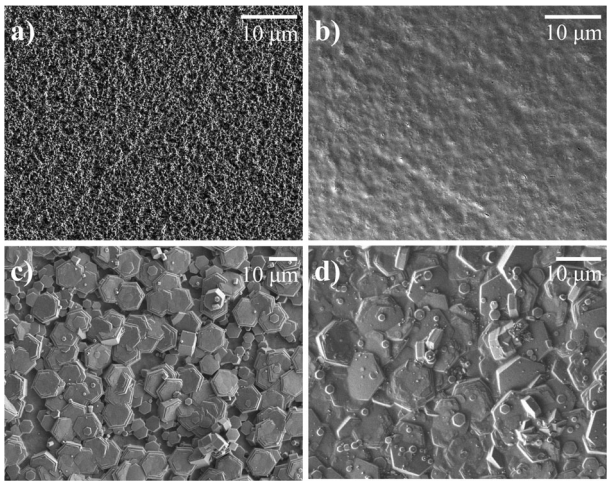

Figure 2. SEM images of a) the bare α-Al_2O_3 support surface and following b) TiO_2 slip-coating, c) in situ hydrothermal microwave CoSAPO-5 growth, and d) secondary hydrothermal microwave growth before heat treatment.

under the conditions studied, a high-quality TiO_2 layer is necessary to produce an oriented seed layer with high surface coverage.

A well-known problem in supported membrane fabrication is the formation of defects which may arise through heat treatment necessary for activation. Notable examples include crack propagation and grain boundary defects in oriented silicalite-1 membranes[4] and thermal densification in $AlPO_4$-5 membranes.[11] SEM visualization of the membrane cross-section (at a tilt angle of 52°) following heat treatment was completed through focused ion beam (FIB) milling. The SEM image in Figure 3a surveys the surface of the heat-treated CoSAPO-5 membrane which is void of observable surface defects or crystal morphology changes when compared to

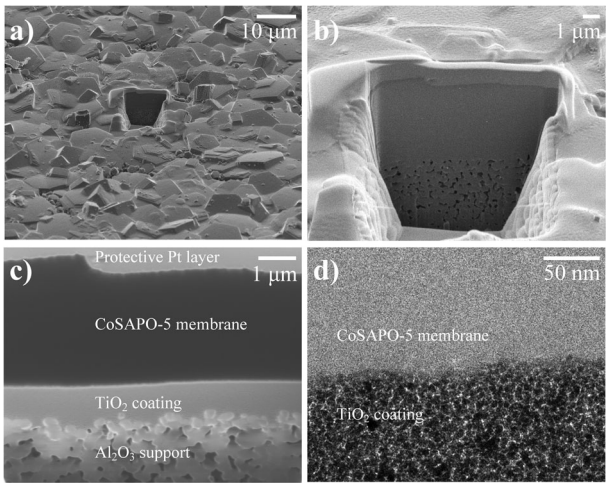

Figure 3. a), b) SEM images of a heat-treated CoSAPO-5 membrane after treatment by focused ion beam milling with a Ga ion source at 40 keV. c) Higher magnification SEM image of (b) identifying the layers comprising the membrane along with d) TEM imaging of the TiO_2 coating/CoSAPO-5 interface. Images in (a–c) were obtained at a tilt angle of 52°.

Figure 2d. SEM imaging in Figure 3b (lower magnification) and 3c (higher magnification) clearly indicates the layers of α-Al_2O_3 support, TiO_2 coating (approximately 1.5 μm thick), and CoSAPO-5 membrane (approximately 5 μm thick) below the protective Pt layer used during imaging. TiO_2 mesoporosity can be seen in the TEM image of the CoSAPO-5 membrane/TiO_2 interface in Figure 3d, which further shows no observable defects in the membrane.

Figure 4a includes representative X-ray diffraction (XRD) patterns for the unsupported CoSAPO-5 powder and the supported membranes. The lower powder pattern

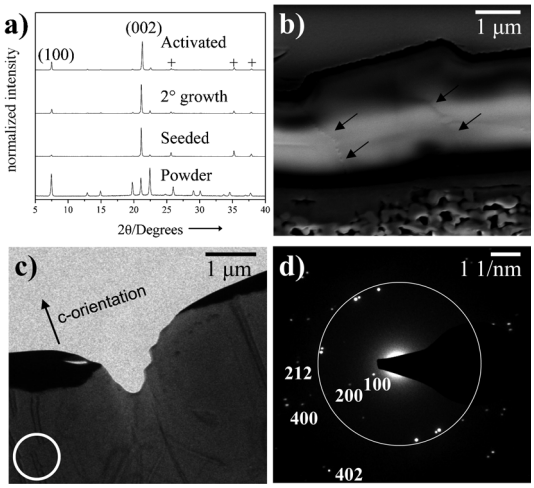

Figure 4. a) XRD patterns of the unsupported CoSAPO-5 powder and supported CoSAPO-5 membranes following in situ hydrothermal microwave growth, secondary hydrothermal microwave growth, and heat treatment. Al_2O_3 support peaks (+) are noted. b) SEM imaging (at a tilt angle of 52°) of the membrane side surface (perpendicular to the crystallographic *c*-axis), with arrows indicating grain features, and c) TEM imaging of a sample prepared by focused ion beam milling with a Ga ion source at 30 keV for d) electron diffraction.

displays a pure AFI phase, indicative of an $AlPO_4$-5 structural analogue. The powder retained the AFI structure at elevated temperatures (up to 550 °C) required to remove the structure-directing agent (Figure S3).[33] Confirmation of preferred *c*-out-of-plane orientation was observed following in situ seeding. Membranes having undergone secondary growth (seen in Figure 2d) sustained the preferential *c*-orientation and showed an increase in intensity relative to the α-Al_2O_3 support peaks, indicating a higher degree of crystalline surface coverage. Recently, it was shown that heating α-Al_2O_3-supported $AlPO_4$-5 or CoAPO-5 membranes to temperatures as low as 400 °C resulted in a structural transformation to a densified $AlPO_4$-tridymite phase, rendering the material incapable for molecular sieving applications.[11] Promisingly, heat treatment of the CoSAPO-5 membrane following secondary hydrothermal microwave growth displayed an XRD pattern (top-most, Figure 4a) consistent with the heat-treated unsupported powder form with no observed transition from the AFI framework type.

Observation of crystal grain structure may be seen in the SEM image in Figure 4b. Arrows indicate vertical features which are grain boundaries. A TEM image of the membrane cross-section following FIB milling is shown in Figure 4c. The electron diffraction pattern in Figure 4d was taken near a region of observed bend contour lines (further TEM images of bend contour features in Figure S4). These bend contours are artifacts of FIB milling, which have been previously reported for perovskite-type membranes.[34] Spot assignment indicates two important details: the absence of (002) when diffracting from the cross-section further confirms crystal orientation, and no peaks were observed which would be assigned to densified $AlPO_4$-tridymite. It may be concluded that the TiO_2-supported CoSAPO-5 membranes are of high-quality and thermally stable to temperatures required for membrane activation.

Permeability measurements using CoSAPO-5 membranes following activation through heat treatment provided a quantitative determination of molecular sieving quality. Noack et al. previously described the alignment of $AlPO_4$-5 crystals in a nickel grid ($AlPO_4$-5-in-nickel) which was further exposed to metal deposition to fill intercrystalline voids.[9] In that work, the pervaporation separation factor, defined as the ratio of permeabilities of *n*-heptane (kinetic diameter 0.43 nm) and 1,3,5-triisopropylbenzene (TIPB, 0.85 nm) through the AFI channels (0.73 nm pore channel opening), was approximately 1200 for an equimolar binary feed. The reported permeability of single component *n*-heptane (1.8×10^{-11} mol m m^{-2} s^{-1} Pa^{-1}), however, was an order of magnitude higher than that in the binary mixture (4.4×10^{-12} mol m m^{-2} s^{-1} Pa^{-1}), indicating a mass transport reduction due to the bulky TIPB molecules blocking the oriented $AlPO_4$-5 pore channel openings. Our first report on the synthesis of 10–20 μm thick $AlPO_4$-5 membranes on porous α-Al_2O_3 showed reduced molecular sieving quality due to crystal densification and defect propagation during high-temperature activation, as exhibited through low separation factors in an equimolar binary feed of *n*-heptane/TIPB regardless of calcination method.[11] From four heat-treated CoSAPO-5 membranes reported here, the *n*-heptane and TIPB single component permeabilities were found to be $3.6 \pm 0.7 \times 10^{-13}$ mol m m^{-2} s^{-1} Pa^{-1} and $8.0 \pm 0.9 \times 10^{-17}$ mol m m^{-2} s^{-1} Pa^{-1}, respectively, giving a separation factor of approximately 4500. The *n*-heptane permeability is lower than expected based on the reported values from the aligned $AlPO_4$-5-in-nickel crystals,[9] while a comparison of the separation factor is similar.

In summary, we demonstrated for the first time the fabrication of highly *c*-oriented, continuous, and homogeneous AFI-type membranes exhibiting high molecular sieving performance. CoSAPO-5 membranes were grown on TiO_2-coated α-Al_2O_3 porous disc supports through in situ and secondary microwave hydrothermal growths. High-temperature membrane activation showed good thermal stability via XRD and electron diffraction, which was further shown by permeability measurements. We are currently investigating whether any improvement in the performance of CoSAPO-5 membranes is possible, focusing on determining the presence of pore blocking of the parallel straight channels, reducing the thicknesses of the TiO_2 or CoSAPO-5 membrane layers, and/or achieving a higher degree of crystallographic orientation.

The quality of the developed AFI-type membranes suggests strong potential in applications such as in biofuel separation, catalysis, sensor design, and host–guest assemblies.

Received: November 15, 2011
Published online: January 27, 2012

Keywords: aluminophosphates · CoSAPO-5 · hydrothermal synthesis · membranes · zeolite analogues

[1] J. Caro, M. Noack, *Microporous Mesoporous Mater.* **2008**, *115*, 215 – 233.
[2] M. E. Davis, *Nature* **2002**, *417*, 813 – 821.
[3] J.-R. Li, R. J. Kuppler, H. C. Zhou, *Chem. Soc. Rev.* **2009**, *38*, 1477 – 1504.
[4] J. Choi, H.-K. Jeong, M. A. Snyder, J. A. Stoeger, R. I. Masel, M. Tsapatsis, *Science* **2009**, *325*, 590 – 593.
[5] Z. Lai, G. Bonilla, I. Diaz, J. G. Nery, K. Sujaoti, M. A. Amat, E. Kokkoli, O. Terasaki, R. W. Thompson, M. Tsapatsis, D. G. Vlachos, *Science* **2003**, *300*, 456 – 460.
[6] J. Hedlund, J. Sterte, M. Anthonis, A. J. Bons, B. Carstensen, N. Corcoran, D. Cox, H. Deckman, W. De Gijnst, P. P. de Moor, F. Lai, J. McHenry, W. Mortier, J. Reinoso, *Microporous Mesoporous Mater.* **2002**, *52*, 179 – 189.
[7] S. T. Wilson, B. M. Lok, C. A. Messina, T. R. Cannan, E. M. Flanigen, *J. Am. Chem. Soc.* **1982**, *104*, 1146 – 1147.
[8] V. Kukla, J. Kornatowski, D. Demuth, I. Girnus, H. Pfeifer, L. V. C. Rees, S. Schunk, K. K. Unger, J. Karger, *Science* **1996**, *272*, 702 – 704.
[9] a) M. Noack, P. Kolsch, D. Venzke, P. Toussaint, J. Caro, *Microporous Mater.* **1994**, *3*, 201 – 206; b) I. Girnus, M.-M. Pohl, J. Richter-Mendau, M. Schneider, M. Noack, D. Venzke, J. Caro, *Adv. Mater.* **1995**, *7*, 711 – 714.
[10] W. Yang, B. Zhang, X. Liu, *Microporous Mesoporous Mater.* **2009**, *117*, 391 – 394.
[11] J. A. Stoeger, C. M. Veziri, M. Palomino, A. Corma, N. K. Kanellopoulos, M. Tsapatsis, G. N. Karanikolos, *Microporous Mesoporous Mater.* **2012**, *147*, 286 – 294.
[12] a) T.-G. Tsai, H.-C. Shih, S.-J. Liao, K.-J. Chao, *Microporous Mesoporous Mater.* **1998**, *22*, 333 – 341; b) T.-G. Tsai, K.-J. Chao, X.-J. Guo, S.-L. Sung, C.-N. Wu, Y.-L. Wang, H.-C. Shih, *Adv. Mater.* **1997**, *9*, 1154 – 1157.
[13] S. Feng, T. Bein, *Science* **1994**, *265*, 1839 – 1841.
[14] W. Yang, X. Liu, L. Zhang, B. Zhang, *Langmuir* **2009**, *25*, 2271 – 2277.
[15] R. Xu, G. Zhu, X. Yin, X. Wan, S. Qiu, *J. Mater. Chem.* **2006**, *16*, 2200 – 2204.
[16] C. M. Veziri, M. Palomino, G. N. Karanikolos, A. Corma, N. K. Kanellopoulos, M. Tsapatsis, *Chem. Mater.* **2010**, *22*, 1492 – 1502.
[17] G. N. Karanikolos, H. Garcia, A. Corma, M. Tsapatsis, *Microporous Mesoporous Mater.* **2008**, *115*, 11 – 22.
[18] G. N. Karanikolos, J. W. Wydra, J. A. Stoeger, H. Garcia, A. Corma, M. Tsapatsis, *Chem. Mater.* **2007**, *19*, 792 – 797.
[19] J.-C. Lin, M. Z. Yates, *Chem. Mater.* **2006**, *18*, 4137 – 4141.
[20] B. M. Lok, C. A. Messina, R. L. Patton, R. T. Gajek, T. R. Cannan, E. M. Flanigen, *J. Am. Chem. Soc.* **1984**, *106*, 6092 – 6093.
[21] D. Tian, W. Yan, X. Cao, J. Yu, R. Xu, *Chem. Mater.* **2008**, *20*, 2160 – 2164.
[22] A. Iwasaki, T. Sano, T. Kodaira, Y. Kiyozumi, *Microporous Mesoporous Mater.* **2003**, *64*, 145 – 153.
[23] T. Kodaira, K. Miyazawa, T. Ikeda, Y. Kiyozumi, *Microporous Mesoporous Mater.* **1999**, *29*, 329 – 337.
[24] G. Finger, J. Richter-Mendau, M. Bulow, J. Kornatowski, *Zeolites* **1991**, *11*, 443 – 448.
[25] V. P. Shiralkar, C. H. Saldarriaga, J. O. Perez, A. Clearfield, M. Chen, R. G. Anthony, J. A. Donohue, *Zeolites* **1989**, *9*, 474 – 482.
[26] S. H. Jhung, J.-S. Chang, D. S. Kim, S.-E. Park, *Microporous Mesoporous Mater.* **2004**, *71*, 135 – 142.
[27] E. Hu, Y. L. W. Huang, Q. Yan, D. Liu, Z. Lai, *Microporous Mesoporous Mater.* **2009**, *126*, 81 – 86.
[28] Y. Yoo, H.-K. Jeong, *Chem. Commun.* **2008**, 2441 – 2443.
[29] X. Li, Y. Yan, Z. Wang, *Ind. Eng. Chem. Res.* **2010**, *49*, 5933 – 5938.
[30] Y. K. Hwang, U.-H. Lee, J.-S. Chang, Y.-U. Kwon, S.-E. Park, *Chem. Lett.* **2005**, *34*, 1596 – 1597.
[31] I. Girnus, K. Jancke, R. Vetter, J. Richter-Mendau, J. Caro, *Zeolites* **1995**, *15*, 33 – 39.
[32] V. T. Zaspalis, W. Van Praag, K. Keizer, J. R. H. Ross, A. J. Burggraaf, *J. Mater. Sci.* **1992**, *27*, 1023 – 1035.
[33] J. W. Richardson, Jr., J. J. Pluth, J. V. Smith, *Acta Crystallogr. Sect. C* **1987**, *43*, 1469 – 1472.
[34] S. Baumann, F. Schulze-Kuppers, S. Roitsch, M. Betz, M. Zwick, E. M. Pfaff, W. A. Meulenberg, J. Mayer, D. Stover, *J. Membr. Sci.* **2010**, *359*, 102 – 109.

